Nonsmoothness, indeterminacy, and friction in two-dimensional arrays of rigid particles

Farhang Radjai and Lothar Brendel
Höchstleistungsrechenzentrum, Forschungszentrum 52425 Jülich, Germany

Stéphane Roux
Laboratoire de Physique et Mécanique des Milieux Hétérogènes,
Ecole Supérieure de Physique et Chimie Industrielles de Paris,
10 rue Vauquelin, F-75231 Paris Cedex 05, France
(Received 7 September 1995)

An algorithm is proposed to simulate regular arrays of perfectly rigid particles with exact Coulomb's law of friction. Relying on this approach, we explore the problems of indeterminacy and dissipation in granular systems. When driven by a basal plane moving at a constant acceleration, a ''steady state'' is achieved where contact forces and angular accelerations of all particles stay constant in time. This state shows a well-defined organization of particle rotations and contact forces. When the driving speed is kept constant, the dissipation rate decreases dynamically to reach its minimum in the steady state. The global frictional behavior of the system can be described in terms of an effective coefficient of friction and an effective inertia. [S1063-651X(96)02907-8]

PACS number(s): 46.10.+z, 83.70.Fn

I. INTRODUCTION

Contact forces in dry granular systems imply two common basic features: steric exclusion and frictional couplings. Steric exclusion means that particles cannot interpenetrate. The process of gain and loss of contacts in the medium and the possibility of lasting contacts to be sliding or nonsliding, are highly nonlinear interactions which directly influence the macroscopic mechanical behavior of the system [1–5].

In the case of *perfectly rigid* particles with *Coulombian friction law*, these nonlinearities take a ''nonsmooth'' form [6–8]. This means, the contact force and the relative displacement at a contact between two particles belong to a continuous set of acceptable values which can not be represented as a function of any of the two variables [9]. Thus, while for elastic contacts the interparticle force at each contact is given locally as a function of the relative displacement, the actual values of contact forces in nonsmooth conditions are determined only when all kinematic constraints in the whole system are explicitly taken into account.

The analytical study of the effects of these nonlinear and nonsmooth interactions on the global behavior of granular systems in deformation is complexified furthermore by two specific features of these systems: *topological disorder* and *particle rotations*. As a result of topological disorder, a particle can have contacts oriented in any direction, and the positions and orientations of contacts are not correlated. On the other hand, rotations of particles and the possibility of the friction force to be more or less ''mobilized'' (i.e., accepts values up to a certain limit where it is ''fully mobilized'') allow for rolling and thus low-dissipative deformation modes for the system. These aspects are absent from the standard continuum theory and motivate much of the recent interest in the discrete approach to the mechanics of granular systems [1,10–14].

The complexity resulting from geometrical disorder suggests that, if the influence of nonlinear interactions is to be explicitly analyzed, regular arrays of particles should be examined in the first place. Such studies can provide insight into the behavior of disordered granular systems. In this paper, we consider regular arrays of rigid disks confined by two flat walls and a basal plane moving with a constant horizontal velocity or acceleration. It is important to emphasize the point that, unlike lattice models, a regular array of rigid disks has no fixed underlying network. Thus starting from a regular geometry the particles can move and the system may evolve to a disordered configuration. Nonetheless, geometrical order can still be preserved for some regions in the space of mechanical parameters. In our model, the relevant parameters are driving acceleration and confining pressure (the pressure applied on the uppermost layer of particles). In this investigation, where the confining pressure is set to zero, we have kept driving accelerations low enough to avoid particle displacements. Hence the internal degrees of freedom are reduced to particle rotations. As we shall see below, even though the particles stay in permanent *geometrical* contact with each other, not all such contacts are force transmitting. Moreover, during the evolution of the system some nontransmitting contacts may turn transmitting and vice versa.

We have set up an original algorithm to simulate this system under nonsmooth conditions. The contact laws and their implementation in the program are discussed in Sec. II. This algorithm provides a vectorial representation of ''contact states.'' Each contact in the medium is force transmitting or nontransmitting, sliding or nonsliding. In the most general case, the system of equations has a unique solution for the contact states, determined at the same time as the contact forces and the angular accelerations of particles. However, in some conditions in statics or in dynamics, the system of equations becomes indeterminate. In contrast with other simulation methods of granular systems, this algorithm allows for a quantitative study of this property, to which Sec. III is devoted.

Our simulations show that the system achieves a ''steady

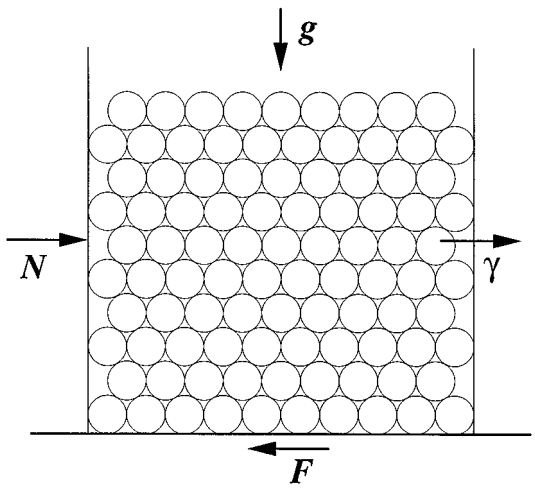

FIG. 1. A schematic representation of the model. The plane is in contact with the first layer of particles. The distance between the two rigid walls is fixed.

state,'' which means that the angular *accelerations* of all particles stay constant in time. In this state, rotation modes give rise to well-defined patterns in the medium. The steady state and the evolution of the system in terms of the global friction on the basal plane and dissipation rate are studied in Sec. IV. Some results can be immediately generalized to disordered systems. Emphasis is put on ''effective inertia'' and the influence of particle rotations on dissipation. A summary of the most important results is presented in Sec. V.

II. THE MODEL AND GOVERNING EQUATIONS

A. The model

Let us consider a regular array of equal-size disks confined by two vertical flat ''walls'' and a plane moving horizontally. Figure 1 shows this geometry with a triangular arrangement of particles. We assume that the particles, the walls, and the plane are *perfectly rigid*. The distance between the two walls is a fixed geometrical parameter which defines the width of the ''box.'' The plane exerts forces on the particles directly in contact with it. The sum of these friction forces is the ''global friction force,'' F_g of the plane on the system. The box, with particles in it, can be considered as a single object moving on the plane. Let N be a horizontal driving force applied on the box. The equation of motion for the center of mass of the whole system is written as

$$N-F_g=m_g\gamma, \tag{2.1}$$

where m_g is the total mass of the system and γ is the horizontal acceleration of the center of mass. If the box were a *solid* closed object (with no particles in it and with a closed bottom), then this equation could be ideally supplemented by the friction law for the sliding contact between the box and plane

$$F_g=\mu_g m_g g, \tag{2.2}$$

where g is the acceleration of gravity and μ_g is the coefficient of friction between the solid and the plane. Thus for a solid box we would solve the two equations to get γ as a function of the driving force and the coefficient of friction. However, in the case of a box filled with particles, the interface between the box and the plane is an array of particles. Some contacts with the plane can be ''nonsliding''(hereafter, NS) and the movement of the plane induces rotations or displacements of the particles in the box, resulting in a bulk dissipation. In these conditions, although Eq. (2.1) still holds for the center of mass of the system, it is not *a priori* clear how the global friction force is related to the particle-plane coefficient of friction and other parameters of the system. Moreover, in the most general case, F_g should depend on the acceleration as well, in which case the inertia of the system could be different from the mass of the system as soon as this dependence is taken into the equation of dynamics. Through this model, we address in fact the central problem raised about granular materials: In what respect are granular systems different from solids? What are the mechanisms that relate the global friction (and dissipation) to the friction at individual contacts?

The key to the analysis is in the organization of the rotations of particles in the system. We consider here the simple situation of regular arrays of particles, where rotation patterns are easier to recognize. Since NS contacts occur very frequently in the system, it is important to incorporate the friction law as accurately as possible. We will consider the *exact* Coulomb's law of friction, which is generally regularized in other simulation methods. Moreover, since steric exclusion seems to dominate the behavior of granular materials in most realistic situations [1–3], we will implement perfectly rigid particles. The mechanical parameters are the particle-particle, particle-plane, and particle-wall coefficients of friction and the applied force N on the box or the acceleration γ of the center of mass. All units can be normalized with respect to the natural quantities of the system. These are the weight and diameter of one particle and the acceleration of gravity.

B. Contact laws

Let p be the number of particles and c the number of contacts. In two dimensions we have $2c$ normal and friction forces to be determined, as well as $3p$ accelerations (corresponding to 2 linear degrees of freedom and 1 angular). Hence the total number of unknowns is $3p+2c$. On the other hand, the number of equations of dynamics is $3p$. Thus $2c$ more equations are needed in order to solve the problem. These equations are given by the interaction laws and, typically, we should have two equations for each contact. For the nonsmooth problem we consider in this paper, these laws are Signorini's condition and Coulomb's friction law, as described below.

1. Signorini's condition

Since we consider perfectly rigid particles, the normal contact forces are not given by local elastic displacements. The contact law is then reduced to a *pure* ''unilaterality'' condition shown by a graph on Fig. 2(a). This graph, known as ''Signorini's condition'' in the context of nonsmooth mechanics, expresses simply that a contact force can be nonzero only if there is a geometrical contact and it can have arbi-

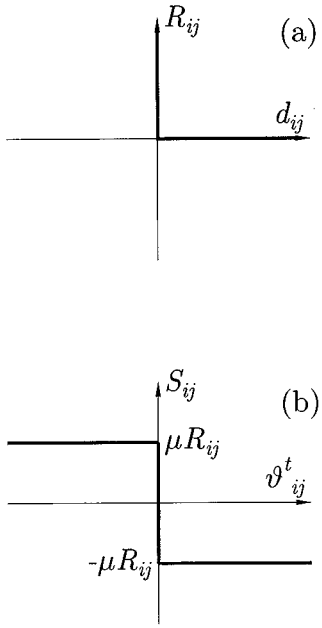

FIG. 2. The graphs of (a) Signorini's condition (b) Coulomb's law of friction. R_{ij} and S_{ij} are, respectively, the normal and tangential components of the contact force between the particles i and j; d_{ij} is the interstice and ϑ^t_{ij} is the tangential relative velocity; μ is the coefficient of friction.

trarily high values to satisfy the condition of noninterpenetrability [6–8]. It is written as

$$d_{ij}=0 \Rightarrow R_{ij} \geqslant 0$$
$$d_{ij}>0 \Rightarrow R_{ij}=0, \tag{2.3}$$

where d_{ij} is the distance between the borders of the two particles i and j (the interstice) and R_{ij} is the normal component of the contact force.

Signorini's condition is *nonsmooth* in the sense that none of the two variables d and R is a function of the other one. The normal force and the interstice belong to a continuous set of acceptable values. We may distinguish, however, between ''stable'' and ''unstable'' contacts. When at a given instant of evolution of the system two particles keep touching each other, the contact is stable. In other words, for a stable contact not only the interstice, but also the relative normal velocity is zero. On the other hand, if the interstice is zero but the relative normal velocity is positive (particles going apart from each other), then the contact is unstable and the reaction force is necessarily zero. In this way, Signorini's condition takes the following form in terms of the interstice and the relative normal velocity:

$$d_{ij}=0 \Rightarrow \begin{cases} \vartheta^n_{ij}=0 & \text{and } R_{ij} \geqslant 0 \\ \vartheta^n_{ij} \geqslant 0 & \text{and } R_{ij}=0, \end{cases} \tag{2.4}$$
$$d_{ij}>0 \Rightarrow R_{ij}=0,$$

where ϑ^n_{ij} is the relative normal velocity between particles i and j.

The highly constraining nature of Signorini's condition appears only when a dynamic system of particles is considered, i.e., when either discontinuous changes of velocities take place due to collisions or stable contacts tend to become unstable due to a nonzero relative normal acceleration. The regular systems we consider in this paper involve no collisions and all contacts are stable. Let us distinguish contacts where the relative normal acceleration $\dot{\vartheta}^n_{ij}$ is zero from the other contacts. Then, we can immediately write Signorini's condition for the relative normal accelerations

$$d_{ij}=0 \Rightarrow \begin{cases} \dot{\vartheta}^n_{ij}=0 & \text{and } R_{ij} \geqslant 0 \\ \dot{\vartheta}^n_{ij} \geqslant 0 & \text{and } R_{ij}=0, \end{cases} \tag{2.5}$$
$$d_{ij}>0 \Rightarrow R_{ij}=0.$$

The difference between Eq. (2.4) and Eq. (2.5) is in the point that the latter is a set of alternative equations for the *dynamic* variables R_{ij} and $\dot{\vartheta}^n_{ij}$. These equations can be supplemented to the equations of dynamics to solve for the forces and accelerations. There are two alternatives:

(1) $\dot{\vartheta}^n_{ij}=0$ and $R_{ij} \geqslant 0$: In this case, the equation $\dot{\vartheta}^n_{ij}=0$ is supplemented to the equations of dynamics, from which the value of R_{ij} can be calculated. If this value satisfies the corresponding inequality $R_{ij} \geqslant 0$, then the solution is acceptable.

(2) $R_{ij}=0$ and $\dot{\vartheta}^n_{ij} \geqslant 0$: In this case, the equation $R_{ij}=0$ should be supplemented to the equations of dynamics, from which the value of $\dot{\vartheta}^n_{ij}$ is calculated. If the corresponding inequality $\dot{\vartheta}^n_{ij} \geqslant 0$ is satisfied the solution is acceptable. Otherwise, we should turn to the other alternative.

In this way, in dynamics the initial inequalities expressing the conditions of unilateral contacts have been replaced by a set of alternative equations (bilateral conditions). In the case of regular systems, the two alternatives correspond to force-transmitting (T) and nontransmitting (NT) contacts, respectively. This process of searching for the mechanically acceptable solution has to be applied simultaneously to all contacts in the system. As we shall see below, except for pathological configurations, the solution for normal forces, accelerations, and normal states (T or NT) of contacts is unique.

2. Coulomb's law of friction

A friction law is a relation between the friction force and the relative tangential velocity at the contact between two particles. The graph of this relation for Coulomb's law is shown on Fig. 2(b). In two dimensions, it is written as

$$\vartheta^t_{ij}=0 \Rightarrow S_{ij} \in [-\mu R_{ij}, \mu R_{ij}],$$
$$\vartheta^t_{ij}>0 \Rightarrow S_{ij}=-\mu R_{ij}, \tag{2.6}$$
$$\vartheta^t_{ij}<0 \Rightarrow S_{ij}=\mu R_{ij},$$

where ϑ^t_{ij} is the relative tangential velocity at the contact ij between the particles i and j, and S_{ij} is the tangential component of the contact force. Here again, we have a nonsmooth condition and the two variables ϑ^t_{ij} and S_{ij} belong to a continuous set of acceptable values. In static equilibrium, where all relative velocities are zero (on the vertical branch

of Coulomb's graph), Coulomb's law results indeed in an indeterminate state of forces (see Sec. III). In the same way, for a given set of friction forces at the sliding limit (on the horizontal branches of Coulomb's graph), the relative tangential velocities are not uniquely determined.

This local indeterminacy is, however, removed as soon as Coulomb's law is associated with the equations of dynamics. There we have to distinguish the contacts where the relative tangential velocity *remains* equal to zero from those where this is not the case. In other words, there are contacts where the relative tangential velocity is equal to zero and contacts where both the relative tangential velocity and acceleration are equal to zero. Only the latter actually stays a nonsliding (NS) contact. Thus at each NS contact ij, there are three different alternatives:

(1) $\dot{\vartheta}^t_{ij}=0$: In this case, the contact stays NS. The friction force S_{ij} has to be in Coulomb's limits $[-\mu R_{ij},\mu R_{ij}]$. Here we have an equation and an inequality. When the equation $\dot{\vartheta}^t_{ij}=0$ is supplemented to the equations of dynamics, we get the value of S_{ij} and we can check for the inequality. If the inequality is satisfied as well, then we have the solution. Otherwise, the force necessary to keep the contact NS exceeds the highest possible value, i.e., the contact starts to slide and we have to switch to one of the two other alternatives.

(2) $\dot{\vartheta}^t_{ij}>0$: In this case, the contact becomes sliding. So, we have to set $S_{ij}=-\mu R_{ij}$ following the sign convention of Fig. 2(b). Here again we have an equation and an inequality. We supplement the equations of dynamics by this equation, from which we calculate $\dot{\vartheta}^t_{ij}$ among others, and we check for the inequality. If the inequality is not satisfied, then we turn to another alternative.

(3) $\dot{\vartheta}^t_{ij}<0$: This is similar to the second case, the corresponding equation being $S_{ij}=\mu R_{ij}$. In this way, Coulomb's law in its most general formulation, takes the following form:

$$\vartheta^t_{ij}=0\Rightarrow\begin{cases}\dot{\vartheta}^t_{ij}=0 & \text{and } S_{ij}\in[-\mu R_{ij},\mu R_{ij}]\\ \dot{\vartheta}^t_{ij}\geqslant 0 & \text{and } S_{ij}=-\mu R_{ij}\\ \dot{\vartheta}^t_{ij}\leqslant 0 & \text{and } S_{ij}=\mu R_{ij},\end{cases} \tag{2.7}$$

$$\vartheta^t_{ij}>0\Rightarrow S_{ij}=-\mu R_{ij},$$

$$\vartheta^t_{ij}<0\Rightarrow S_{ij}=\mu R_{ij}.$$

We recall that in most numerical simulations of granular systems ''regularized'' forms of Signorini's condition and Coulomb's law are implemented. Thus, the vertical branches of the graphs are replaced by straight lines with finite slopes which can either be adjusted in order to optimize computation or to model an elastic contact law. A ''contact model'' is, indeed, necessary when the phenomena of the contact scale (small time intervals and deformations as compared to the sizes of particles and interstice and the characteristic time of successive events in the medium), such as the propagation of sound, are to be considered.

C. Governing equations

The algorithm we propose for the simulation of perfectly rigid particles with frictional couplings is directly inspired by the reformulation of contact laws in terms of alternative equations. In order to solve the system, the alternative configurations are to be tested successively until the solution is found. This has to be done simultaneously for all contacts.

We write the equations of dynamics for a given set of contact states. Each contact is either sliding or nonsliding (NS), force-transmitting or nontransmitting (NT). For a NT contact (ij), we simply write

$$R_{ij}=0. \tag{2.8}$$

For a transmitting contact, the relative normal acceleration is set to zero. From the equations of dynamics, this implies the following equation for the forces acting on the two particles i and j in contact:

$$\frac{1}{m_i}\sum_k (R_{ik}\boldsymbol{n}_{ik}\cdot\boldsymbol{n}_{ij}+S_{ik}\boldsymbol{t}_{ik}\cdot\boldsymbol{n}_{ij}) - \frac{1}{m_j}\sum_l (R_{jl}\boldsymbol{n}_{jl}\cdot\boldsymbol{n}_{ij}+S_{jl}\boldsymbol{t}_{jl}\cdot\boldsymbol{n}_{ij}) = -\left(\frac{\boldsymbol{F}_i^{\text{ext}}}{m_i}-\frac{\boldsymbol{F}_j^{\text{ext}}}{m_j}\right)\cdot\boldsymbol{n}_{ij}-(r_i+r_j)\Omega_{ij}^2, \tag{2.9}$$

where m_i and r_i are the mass and radius of particle i, respectively, and $\boldsymbol{F}_i^{\text{ext}}$ is an external force applied on particle i. The local frame is represented by the two unitary vectors $\boldsymbol{n}_{ij}$ and $\boldsymbol{t}_{ij}$. The angular velocity of the contact normal Ω_{ij} is zero for a regular array. The two indices k and l represent the particles in contact with i and j, respectively.

If a contact is sliding, we have the equation

$$S_{ij}=-\text{sgn}(\vartheta^t_{ij})\mu R_{ij}. \tag{2.10}$$

If it was NS but becomes sliding, the equation is similar

$$S_{ij}=-\text{sgn}(\dot{\vartheta}^t_{ij})\mu R_{ij} \tag{2.11}$$

and when it stays NS, the relative tangential acceleration is zero and we get the following equation:

$$\frac{1}{m_i}\sum_k (R_{ik}\boldsymbol{n}_{ik}\cdot\boldsymbol{t}_{ij}+S_{ik}\boldsymbol{t}_{ik}\cdot\boldsymbol{t}_{ij}) - \frac{1}{m_j}\sum_l (R_{jl}\boldsymbol{n}_{jl}\cdot\boldsymbol{t}_{ij}+S_{jl}\boldsymbol{t}_{jl}\cdot\boldsymbol{t}_{ij})+\frac{r_i^2}{I_i}\sum_k S_{ik}+\frac{r_j^2}{I_j}\sum_l S_{jl} = -\left(\frac{\boldsymbol{F}_i^{\text{ext}}}{m_i}-\frac{\boldsymbol{F}_j^{\text{ext}}}{m_j}\right)\cdot\boldsymbol{t}_{ij}. \tag{2.12}$$

It is interesting to separate the terms in Eqs. (2.9) and (2.12) for which $k=j$ and $l=i$, which leads to

$$\dot{\vartheta}^n_{ij}=\left(\frac{1}{m_i}+\frac{1}{m_j}\right)R_{ij}+A^n_{ij} \tag{2.13}$$

$$\dot{\vartheta}^t_{ij}=\left(\frac{1}{m_i}+\frac{1}{m_j}+\frac{r_i^2}{I_i}+\frac{r_j^2}{I_j}\right)S_{ij}+A^t_{ij}. \tag{2.14}$$

These are the equations of dynamics formulated in the local frame, where A^n_{ij} and A^t_{ij} denote the contributions from other contacts and external forces. Actually these terms are responsible for the nonlocal character of the problem.

All together, Eqs. (2.8) or (2.9) and (2.10), (2.11), or (2.12) define a system of linear equations for the forces R_{ij} and S_{ij}, written shortly as

$$\boldsymbol{Mx}=\boldsymbol{b}. \tag{2.15}$$

The vector $\boldsymbol{x}$ consists of the unknown contact forces while the matrix $\boldsymbol{M}$ contains mainly information on geometry (angles between local frames) and states of contacts. The right hand side $\boldsymbol{b}$ is built of the external and inertial forces.

The angular accelerations of particles are computed from contact forces for the set of contact states. However, these forces and accelerations should fulfill the inequalities (2.5) and (2.7) set by contact laws. If this is not the case for all contacts, then a new set of contact states has to be tried. The choice of the alternative set of states is guided naturally by the states of those contacts where the inequalities are not satisfied. This process is iterated until the solution is found.

The evolution of a granular system in nonsmooth conditions is characterized by discontinuities in velocities (due to collisions) or in accelerations and contact forces (due to Coulombian friction). In regular systems only friction can induce ''jumps'' of forces and accelerations whenever an ''event'' occurs (vanishing of the relative tangential velocity on a contact). The event can be located on a single contact. Nevertheless, it may cause some NS contacts to become sliding or some T contacts to change to NT (and vice versa) at the same time.

In the simulations we present in this article, the motion is ''smooth'' between two successive events. The algorithm determines the exact moment of each event. The new values of variables are calculated at this moment according to the iterative scheme of testing alternative equations. Then the system is evolved again. The convergence to the solution takes place only in a few iterations, unless the system of equations is indeterminate, in which case a particular solution has to be found.

III. INDETERMINATE STATES

Indeterminacy of the state of forces arises in the analysis of structures composed of rigid elements. It is shown that, in many problems, the number of forces to be determined is greater that the number of equations of static equilibrium and the constraints. Such indeterminacies are, however, removed by supplementing the equilibrium equations with additional equations pertaining to the displacements of the structure [15].

In this section, we study the indeterminacy arising in regular arrays of rigid particles. We begin with a general introduction to the problem. Then, we show how the techniques of ''singular value decomposition'' can be used in our simulations to determine the degree of indeterminacy and the contacts contributing to it. Finally, we identify the geometrical constraints at the origin of indeterminacy and we discuss possible solutions to the problem.

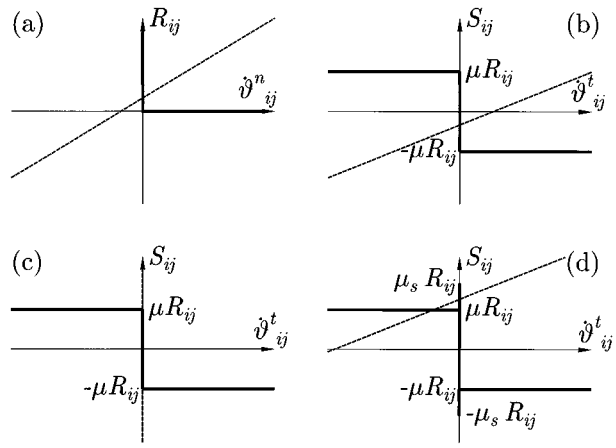

FIG. 3. (a) and (b). The equations of dynamics [cf. Eqs. (2.13) and (2.14)] projected on the local frame, attached to a contact between two particles, are shown as (dashed) straight lines with positive finite slopes. These cut Coulomb's and Signorini's graphs at a single point. (c) In static equilibrium, the slope is formally infinite (since $\dot{\vartheta}^t_{ij}$ is kept zero) and the intersection with the two graphs is multiple valued. (d) When a friction law involving static and dynamic thresholds is considered, the solution is no more unique.

A. Uniqueness and indeterminacy

In dynamics, the local nonsmoothness in the friction law does not by itself result in indeterminacy. The general argument in favor of uniqueness of the solution in a dynamic system of particles is shown in Fig. 3(b). For each contact, the friction force satisfies Coulomb's graph. On the other hand, the equation of dynamics stated in the local frame attached to a contact, turns out to be a straight line with a finite positive slope [cf. Eqs. (2.13) and (2.14)]. The intersection between this line and Coulomb's graph is a single point which gives a unique value for the friction force at that contact. In statics, the relative tangential acceleration is zero and the straight line representing the equation of dynamics in the local frame is simply a vertical line going through the origin. This line covers the whole vertical branch of Coulomb's graph and, thus, the friction force at the contact stays indeterminate [Fig. 3(c)].

The same argument applies also to Signorini's graph [see Fig. 3(a)]. From this it becomes clear that uniqueness of the solution is also due to the form of the basic Coulomb's law. For instance, if besides the dynamic coefficient of friction a static threshold is introduced into this graph, then there can be two solutions for each contact at the same time and the actual value of the friction force depends on the history of the system [Fig. 3(d)].

In static equilibrium, we never have enough equations to solve the system of equations. Let c and p be the number of contacts and the number of particles in a granular system, respectively. There are $2c$ forces to be determined (the accelerations are set to zero). But we have $3p$ equations of equilibrium. Since in a disordered medium the mean number of contacts is about two times that of particles [16], the total

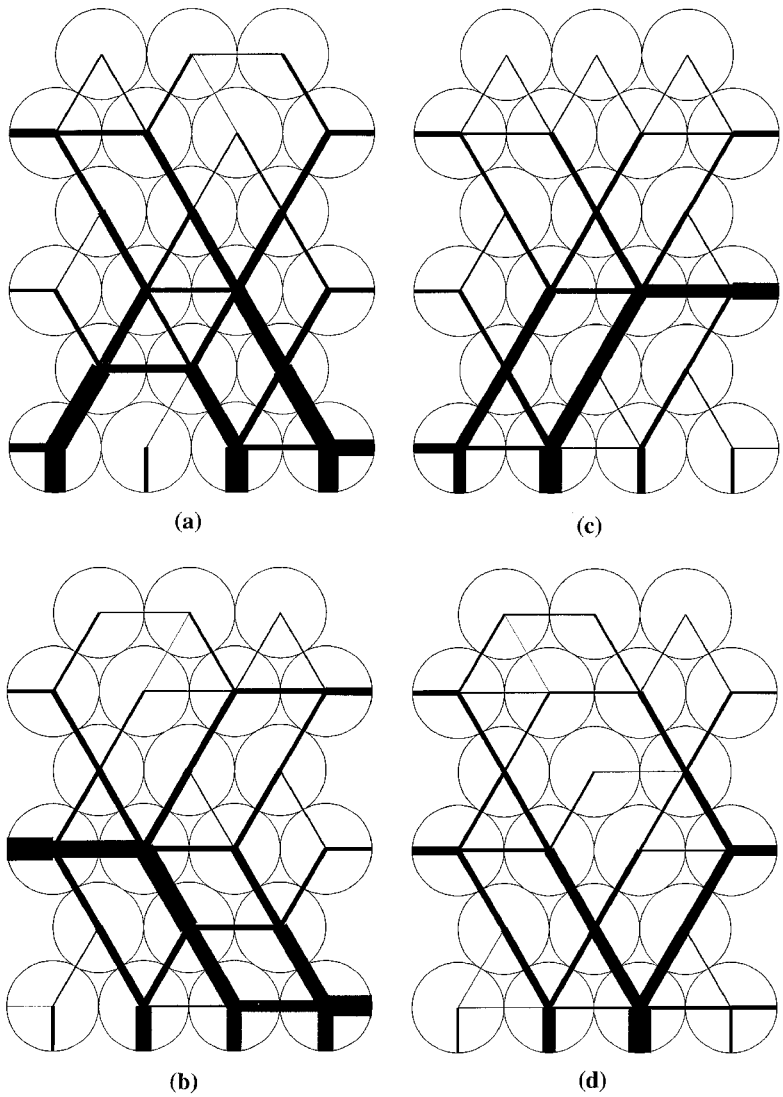

FIG. 4. Four different solutions for the normal contact forces in a triangular assembly. The widths of intercenter segments are proportional to the corresponding contact forces. Particles have different angular velocities (positive and negative). They are kept the same in the four configurations.

number of forces to be determined is $4p$. In this way, there are p undetermined forces in the system. In other words, in static equilibrium, half of the friction forces are undetermined.

We note that this is a *bulk indeterminacy*, for the degree of indeterminacy is of the same order of magnitude as the size of the system. One important implication of this situation is that the indeterminacy cannot be removed just by controlling forces on the boundary, whose contribution to the total indeterminacy is only proportional to the total surface of the boundary in terms of the number of particles. It is then an interesting and highly nontrivial question to know how the friction forces are distributed inside a disordered granular system, in particular in the limit of macroscopic ''failure.''

B. Singular value decomposition

The contact matrix $\boldsymbol{M}$, introduced in Sec. II, contains all the information about the states and orientations of contacts. If this matrix is singular, then the system of equations is indeterminate and the dimension of the null space gives the degree of singularity. One solution, among an infinite number of solutions, can be singled out by setting mechanically acceptable values of as many contact forces as the degree of singularity, otherwise the states of some contacts can be changed in order to set up a new contact matrix. Figure 4 shows four different solutions of forces for the same system with the same boundary conditions. In this example, the tangential contact states are set to be sliding at all contacts and only normal contact states change.

We have used the ''singular value decomposition'' (SVD) to study the singularities of the contact matrix [17]. Based on a general theorem of linear algebra, SVD allows to decompose the matrix $\boldsymbol{M}$ as follows:

$$\boldsymbol{M}=\boldsymbol{U}\cdot[\mathrm{diag}(w_{ii})]\cdot\boldsymbol{V}^T, \tag{3.1}$$

where $\boldsymbol{U}$ and $\boldsymbol{V}$ are two orthogonal matrices and the elements w_{ii} (the singular values) are positive or zero. The columns i of $\boldsymbol{U}$ such that $w_{ii}\neq 0$ form an orthonormal set of basis vectors that span the range of the matrix $\boldsymbol{M}$. The columns i of $\boldsymbol{V}$ such that $w_{ii}=0$ form an orthonormal basis for the null space.

What is the connection between the basis of the null space, obtained explicitly from the SVD, and contact states? Each line α of the contact matrix corresponds to an equation implying the contact labeled α. Let $\{\boldsymbol{e}^{\alpha}\}$ be the unitary or-

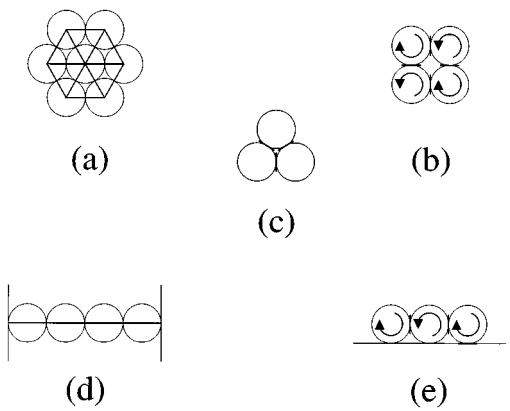

FIG. 5. Different basic structures contributing to the indeterminacy of solutions resulting from the normal contact states (a) and (d) or from the tangential contact states [(b), (c), and (e)].

thonormal basis. If $\boldsymbol{e}^{\alpha}$ is orthogonal to the null space, then the contact α does not contribute to the singularity of the matrix $\boldsymbol{M}$. In other words, the condition for a contact α not to contribute to the singularity is written as

$$\boldsymbol{e}^{\alpha}\cdot\boldsymbol{v}^{\beta}=0 \quad \text{for all} \quad \beta, \tag{3.2}$$

where $\{\boldsymbol{v}^{\beta}\}$ is a basis of the null space. To each basis vector of the null space corresponds a group of contacts contributing by one degree to the total degeneracy of equations.

Let us first consider the normal contact state, which sets the state of a given contact to be T or NT. The singularities can arise only from transmitting contacts. Indeed, from the point of view of equations a NT contact does not ''exist,'' since for such a contact the two components of the contact force are both zero. On the other hand, the maximum number of singularities can occur in a system whose contacts are all transmitting. We have studied the number of singularities due to the normal contact state in triangular and rectangular arrays. The number of singularities is given by

$$N_n=\begin{cases} L_xL_y-2L_y+2 & \text{triangular} \\ L_y & \text{rectangular,} \end{cases} \tag{3.3}$$

where L_y is the number of rows and L_x is the number of particles in a row (in the triangular case L_x is the number of particles in rows which are in contact with the two walls of the frame).

We note that in the triangular assembly, the degree of singularity has a bulk term which is of the same order of magnitude as the number of particles in the system. This is a specific feature of the triangular arrangement. Indeed, let us consider the six neighboring particles of a given particle in the medium. These particles form a regular hexagon around the central particle [Fig. 5(a)]. Each particle of this hexagon has one contact with the central particle and two contacts with its lateral neighbors. However there is one degree of redundancy in the preceding statement. Because, given all contacts of the particles in the hexagon with the central particle and five lateral contacts, the existence and position of the last lateral contact can be geometrically predicted. Since this argument applies to each particle in the medium independently of other particles, we can conclude that the degree of singularity resulting from these geometrical constraints in the bulk is one per particle. This is in agreement with Eq. (3.3) obtained from our simulations. Moreover, in our vectorial representation of the states of contacts through the contact matrix, to each group of 12 contacts defined by one particle and its six neighbors corresponds one basis vector of the null space. For particles in contact with the rigid walls of the frame, an analogous study yields the corresponding contribution to the total singularity. This contribution is only proportional to the total surface of the boundary.

In the rectangular assembly, according to Eq. (3.3), there is one degree of singularity per row. In fact, each row is limited by two rigid walls [Fig. 5(d)]. Given the distance between the two walls, which is an integer multiple of one particle diameter, existence and the exact position of one contact can be predicted from the positions of all the other contacts in each row. This situation results in one degree of singularity in the system of equations for each row. Hence the set of lateral contacts in each row represents a basis vector of the null space. This configuration of particles forming a row in contact with the two walls exists also in the triangular arrangement and contributes to the total singularity.

Another source of singularities of the contact matrix is the configuration of tangential contact states. In this case, only nonsliding (NS) contacts can result in redundancy. For sliding contacts the contact equation is local, that is the friction force is given as a function of the normal force at the same contact, so that it cannot be a linear combination of equations associated with other contacts. Hence the maximum degree of singularity happens when a maximum number of contacts are NS. This is particularly the case when the rotation velocities of all particles are zero. Then the degree of degeneracy is given by

$$N_t=\begin{cases} 2L_xL_y-2L_y-L_x+2 & \text{triangular} \\ L_xL_y+L_y & \text{rectangular.} \end{cases} \tag{3.4}$$

Geometrically, each loop of a minimal number of particles contributes by one degree to the total degeneracy. The basic configuration for the rectangular lattice is a loop of four particles shown in Fig. 5(b). If three of the contacts are NS, then the fourth contact is necessarily NS. Since each particle is common to four loops of four particles, the degree of singularity is one per particle for the rectangular array. This is in agreement with Eq. (3.4), where the bulk term is almost equal to the number of particles. In the case of triangular arrays, the same argument applies for a loop of three particles [where rotation is generically frustrated, cf. Fig. 5(c)]. Here six loops belong to each particle, while each loop in turn is shared by three particles. This results in two degrees of singularity per particle in agreement with Eq. (3.4).

For the tangential contact state too, the contacts with the boundary may contribute to the total singularity. Figure 6 shows the initial angular velocities of an array of seven particles on a flat plane. The angular velocities are also shown at some stage of evolution of the system, where the system of equations is indeterminate due to the rotation mode of particles. Indeed, some particles are rotating alternatively in two opposite directions. Those rotating in the positive direction (the same direction as the linear motion of the particles) are

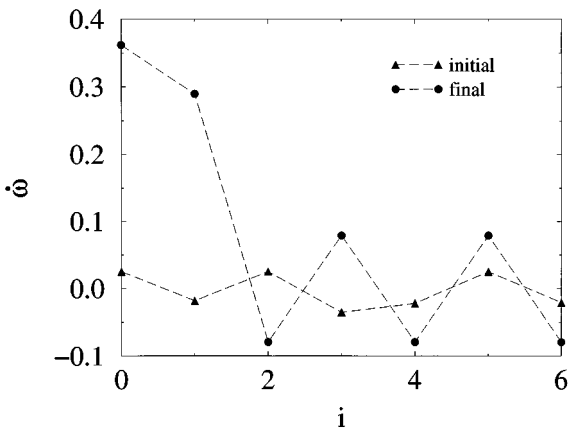

FIG. 6. Rotation velocities of seven particles moving on a plane. The initial random distribution of velocities evolves to a particular indeterminate mode. All quantities are normalized with respect to the weight and radius of one particle and the acceleration of gravity. The particle-particle and particle-plane coefficients of friction are both 0.3.

also rolling on the plane. This mode implies a loop of four NS contacts, which are shown in Fig. 5(e), and are at the origin of indeterminacy of the system, although the system is not in static equilibrium. This particular mode happens whenever the plane-particle coefficient of friction is sufficiently high.

It is important here to emphasize the point that Eq. (3.4) gives the maximum number of singularities in statics. In dynamics, the number of singularities is always smaller. The loop of four contacts remains in any case the basic independent representation of the basis vectors of the null space.

We recall that the basic structures of Fig. 5 contributing to the total singularity of the system of equations correspond to a particular basis of the null space. Other more complex structures can be chosen instead. In other words, the basis of the null space can be set up differently. Each basis singles out a different set of contact configurations.

C. Particular solutions

In Sec. III B, we have identified the geometrical and kinematic constraints giving rise to indeterminate states in two dimensions. The singularities can be removed by choosing as many sliding and nontransmitting contacts as possible. The restriction on the number of such contacts comes from the mechanical acceptability of the states. In fact, a random choice of contact states leads most of the time to unacceptable situations. These are situations where the evolution of the system would result in interpenetration of particles or in a friction force incompatible with Coulomb's law.

An example of a mechanically acceptable solution (among an infinite number of other solutions) in the triangular assembly is the one where all transmitting contacts are sliding and all lateral contacts (contact normals oriented horizontally) are NT. This could be the physical solution for contact states when the whole system is vertically compressed. The total number of lateral contacts is $N_l = L_x L_y - L_y/2$, where the number of rows is taken to be even. The total number of lateral NT contacts is thus greater than the maximum degree of indeterminacy. Depending on the angular velocities of particles, still more contacts could be NT in this configuration.

As emphasized above, in nonsmooth conditions, an acceptable solution implies all kinematic constraints in the whole assembly to be taken into account. A practical consequence of this property is that the preparation of a pile is always a collective operation even when a step-by-step procedure is used. Starting with one grain and adding grains one by one according to a well-defined procedure, does not necessarily lead to a packing of the desired properties. The addition of each grain can modify the configuration or contact states obtained in the preceding steps. This is more particularly the case at macroscopic instability thresholds, where big events can be triggered by the addition of one grain. This nonlocality is manifest in two characteristics of the distribution of forces inside a granular medium: strong-force paths and arching. Both of these phenomena can be observed in Fig. 4 obtained from *random* distributions of normal contact states. Along such structures, a small modification of the state of one contact can result in long-range reorganization of contact states.

The geometrical property at the origin of bulk indeterminacy due to normal contact states is irrelevant to real granular media, where particles have different shapes and sizes. This seems to be usually true for tangential contact states, too. For example, a loop containing an even number of NS contacts implies no redundant information. Indeed, since the sizes of particles are different and they can move, the fact that all contacts in the loop are NS provides the new information that at least two particles are moving. However, the indeterminacy due to tangential contact states is still relevant to disordered granular systems in static equilibrium and probably, for some configurations, in dynamics. This is the most important singularity and, as mentioned in Sec. III A, concerns half of the contacts inside the medium in static equilibrium.

IV. EVOLUTION OF CONTACT STATES

The evolution of a granular system in nonsmooth conditions is essentially that of contact states. Contact forces, angular accelerations, and dissipation rate undergo a discontinuous change every time a contact in the medium changes its state. Relying on the numerical scheme described above, we have studied some aspects of the evolution for rather small systems of particles.

A. Self-organization and modes

Our simulations show that, for a given linear acceleration of the box with respect to the basal plane, the whole system achieves a *steady state* where the relative tangent acceleration at every contact has the same sign as the the relative tangent velocity, or both are zero. In the steady state, the angular accelerations of all particles and the contact forces stay constant in time, since the contact states can no more evolve. What is more, this state is independent of the initial angular velocities of particles. Figure 7 shows the angular accelerations of particles in a rectangular array at three different stages of evolution. Figure 8 shows angular accelera-

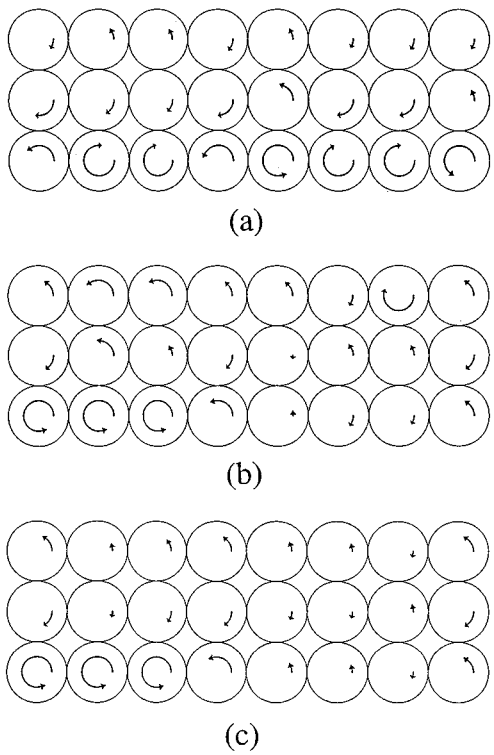

FIG. 7. Angular accelerations of particles at three stages of evolution of a rectangular array. The final stage is the steady state, where the accelerations do not evolve any more. The whole system has a translational acceleration of 0.1 g to the left with respect to the plane. The interparticle and particle-plane coefficients of friction are 0.1 and 0.2, respectively. The coefficient of friction with the walls is zero.

tions, normal forces, and friction forces in the steady state for a rectangular array moving with a constant acceleration of 0.2 g.

The interesting feature of the steady state is the well-defined organization of particle rotations (and equivalently, the contact states). In Fig. 8, three different modes can be distinguished. All particles of the first row (from below) are just rolling on the plane. They have the same angular acceleration and all particle-plane contacts are NS. We will refer to this mode of collective rotation as mode 1. In other rows, the particles rotate still in the same direction, but the angular acceleration decreases in absolute value along the row (mode 2). All lateral contacts between the particles in each row are sliding. Finally, in each column the particles rotate with the same speed but alternatively in the positive and negative directions ($\omega_i = -\omega_j$) except for the particle in contact with the plane (mode 3). All contacts in each column are NS (except for the contacts between the first and second rows).

The same collective modes may appear successively along a column or a row. Figure 9 shows the steady-state angular accelerations for a 10×4 rectangular system as a function of the positions of particles in each row. In the first row (in contact with the plane), there are four particles in mode 1, three particles in mode 2, and two particles in mode 3. The particles in contact with the wall have a particular status, since the walls cannot ''rotate.'' Along other rows a more complicated pattern is observed. However we can still distinguish modes 2 and 3. Mode 3 governs the rotations along columns.

An analytical study of the origin of these modes in a one-dimensional array can be found in Refs. [18,19]. In mode 1, the friction force between the particles and the plane is progressively mobilized along the row [see Fig. 8(c)]. For the last particle in mode 1, the friction force with the plane is fully mobilized and these contacts cannot keep their NS states. There begins mode 2, where the particles are sliding and rotating at the same time. However, the angular acceleration decreases until, for the first particle in mode 3, it becomes negative. From this point, the particles rotate alternatively in positive and negative directions or do not rotate at all. In the particular case where the driving acceleration is set to zero (see below), we observe the same patterns of rotations, except that mode 2 disappears and mode 3 is dominant.

Experiments on granular media show the existence of a ''mesoscopic'' length scale in between the system size and the size of the particles [20]. However, the mechanisms behind these length scales are not well known. Our results suggest one possible mechanism for the appearance of mesoscopic scales: a progressive mobilization of friction forces inside the medium up to the sliding limit.

B. Global friction

A relevant macroscopic quantity is the ''global coefficient of friction'' μ_g on the plane. This is the ratio of the total friction force on the plane to the total weight of the particles. Its time evolution is shown in Fig. 10 for a rectangular array of particles starting with four different initial conditions. Its steady-state value is independent of the initial conditions and depends only on the mechanical parameters of the system.

The global steady-state friction force F_g on the plane varies with the linear acceleration of the system as shown in Fig. 11. It increases linearly with γ when the latter is small. After a nonlinear transition, the dependence again becomes linear with a different slope (namely, zero). In these linear regimes, it is sensible to define an ''effective inertia'' by $m_g + \partial F_g/\partial\gamma$. However, the dependence $F_g(\gamma)$ is in general nonlinear. We introduce the Legendre transformation of $F_g(\gamma)$ which allows us to part in a unique way the friction force in an ''effective inertia'' and an ''effective friction force.'' Let us define two variables a and b by

$$a = \frac{\partial F_g}{\partial \gamma}, \qquad b = F_g - a\gamma. \tag{4.1}$$

Then, Eq. (2.1) can be written in the following form:

$$N - F_e = m_e \gamma, \tag{4.2}$$

where $F_e = b$ and $m_e = m_g + a$ are the effective friction force and effective inertia of the system. Figure 12 shows the variation of the ''effective coefficient of friction'' $\mu_e = F_e/m_g$ and m_e as a function of γ. The former increases with the linear acceleration γ. For high enough values of the linear acceleration, the effective coefficient of friction is al-

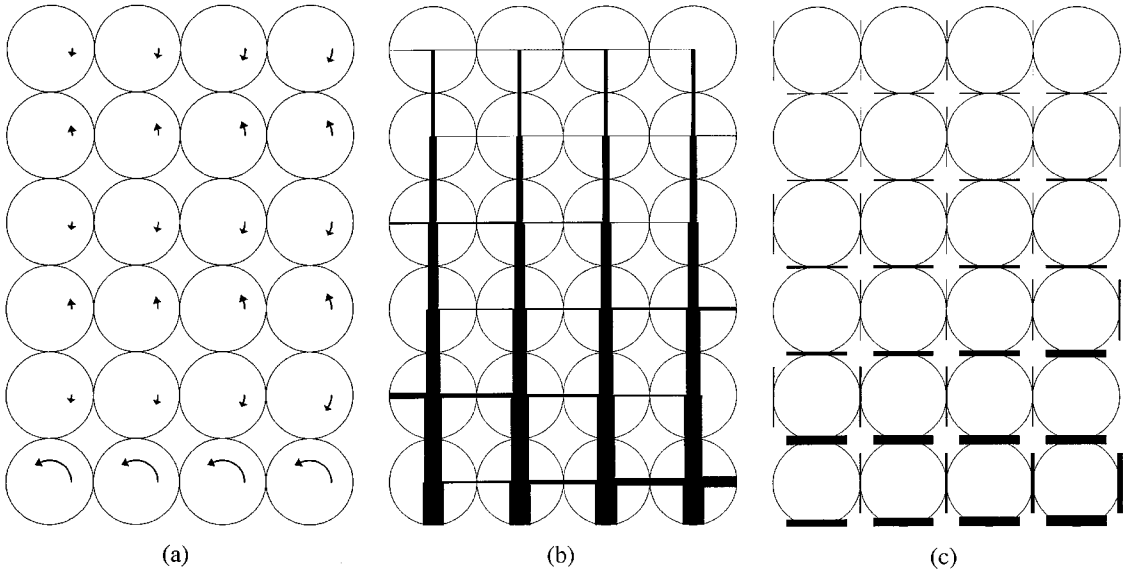

FIG. 8. Steady-state angular accelerations of particles (a), normal contact forces (b), and friction forces (c) of a rectangular array. The whole system is moving with a constant acceleration of 0.2 g to the left with respect to the plane. The interparticle, particle-plane, and particle-wall coefficients of friction are 0.05, 0.2, and 0, respectively.

most equal to the particle-plane coefficient of friction, while the effective inertia is equal to the mass of the system. On the other hand, in the limit of small accelerations, the effective coefficient of friction is very small, while the effective inertia can be many times the real mass of the system.

The behavior of the system in the linear regimes can be understood as follows: For low accelerations gravity plays a more important role than the inertial forces, which leads to mode 3 dominating in each column and mode 1 along each row. Therefore the energy given to the system is barely dissipated (not at all at the plane) but transformed into rotational energy of the grains. Thus we see a low effective friction but a high effective mass. In the regime of high acceleration the situation is reversed: Now inertial forces are important, so mode 3 dominates along the rows, causing frustration of rotation. Hence the system behaves more ''blocklike'' i.e., $\mu_e = \mu_g = \mu_{\text{particle-plane}}$ and there is no additional inertia.

C. Dissipation

We have studied the special case of zero acceleration (i.e., constant velocity of the basal plane) separately. In this case, ''steady state'' refers to the usual sense of constant (angular) velocities. Since constant driving velocity is the limiting case of low driving acceleration, the reached state shows columns in mode 3 and rows in mode 1, as described above. It is interesting that in this case of constant velocity, the self-organization of particle rotations and contact forces, in the

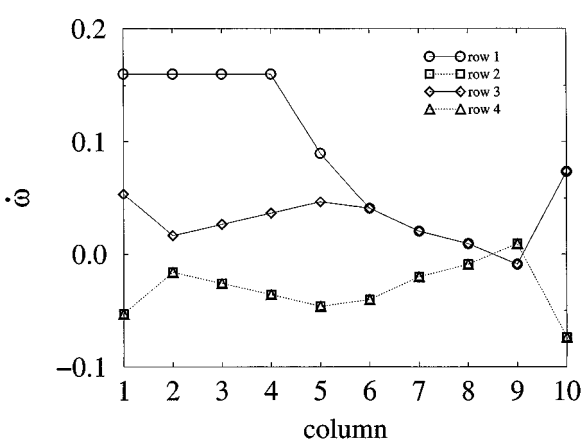

FIG. 9. Steady-state angular accelerations of particles in the first four rows of a 10×4 rectangular array as a function of the particle positions in each row. The array is moving with a constant acceleration of 0.16 g to the left. The interparticle, particle-plane, and particle-wall coefficients of friction are 0.1, 0.2, and 0, respectively. The accelerations are normalized with respect to the acceleration of gravity.

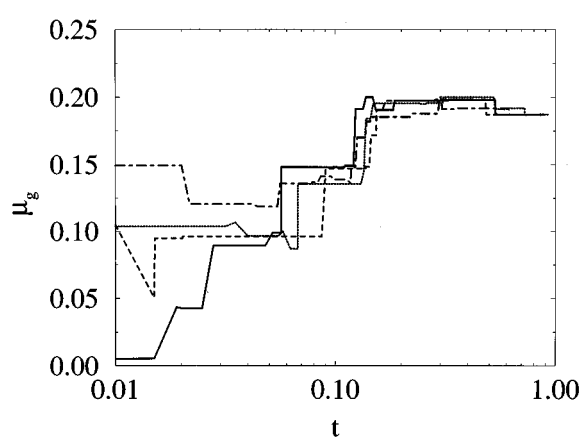

FIG. 10. Evolution of the global coefficient of friction of a rectangular 10×2 array of particles in time starting with four different initial states. The constant driving acceleration is 0.3 g, coefficients of friction for particle particle, particle plane, and particle wall are 0.1, 0.2, and 0, respectively.

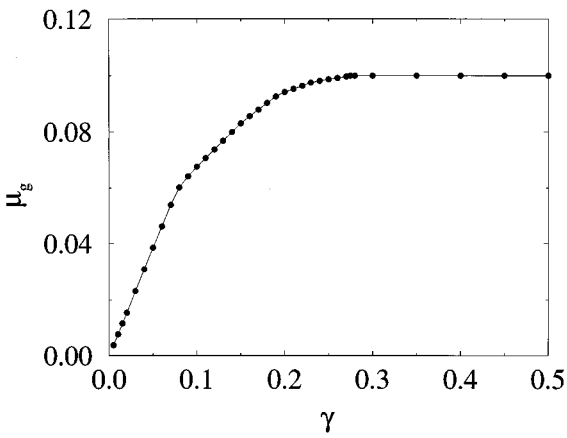

FIG. 11. Global coefficient of friction of a rectangular array as a function of the linear acceleration of the system expressed in the unit of the acceleration of gravity. The interparticle, particle-plane, and particle-wall coefficients of friction are 0.05, 0.1, and 0, respectively. All quantities are normalized with respect to the weight and radius of one particle and the acceleration of gravity.

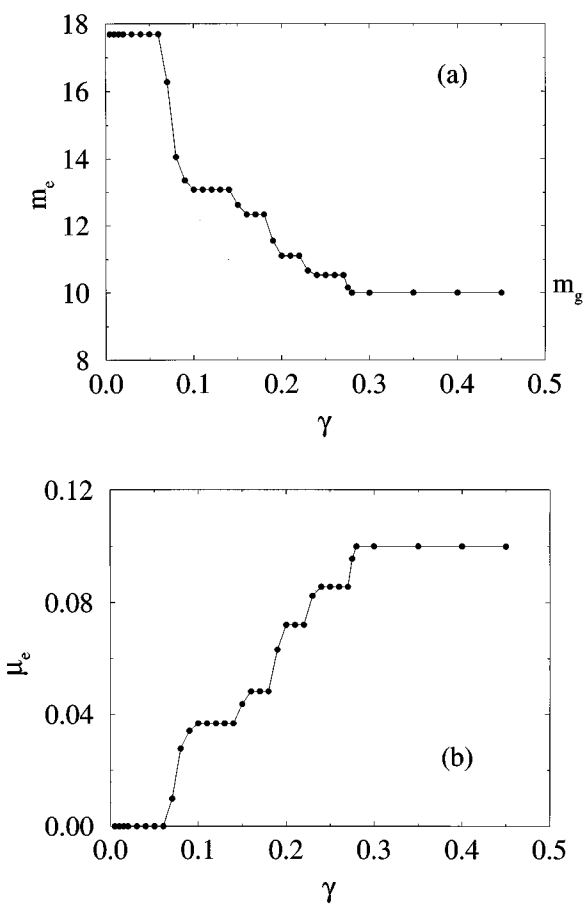

FIG. 12. (a) Effective inertia and (b) effective coefficient of friction as a function of the linear acceleration for the system of Fig. 11. The total mass of the system is $m_g = 10$.

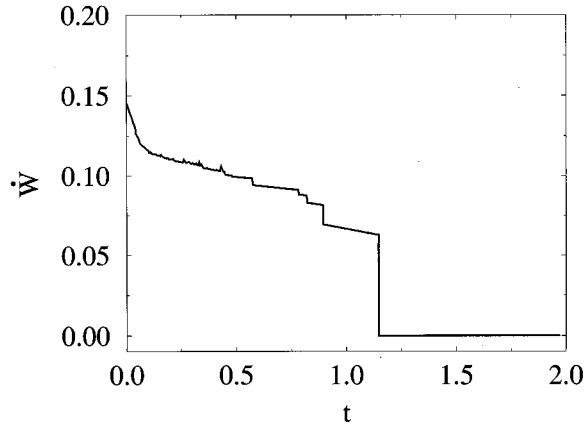

FIG. 13. Total dissipation rate ($\dot{W} = \Sigma_{\langle ij \rangle} S_{ij} \vartheta_{ij}^t$) as a function of time for a rectangular array (10×3) driven with a constant velocity. All quantities are normalized with respect to the weight and radius of one particle and the acceleration of gravity.

sense defined above, results in a very low steady-state dissipation rate. This can be seen in Fig. 13 which shows the evolution of the total dissipation rate for a rectangular array. The steady state appears to be the least dissipative state of the system. The fact is that, due to friction the relative velocities of particles at interparticle contacts tend to decrease. In this way, starting with sliding contacts, many contacts are gradually trapped on the vertical branch of Coulomb's law. The dissipation rate decreases due to this increase of the number of NS contacts. In the rectangular system of Fig. 13 all contacts (except the ones to the walls) finally turned NS. In a triangular system, some frustration of rotations persists, so that the steady-state dissipation rate can be higher as compared to a rectangular system with the same parameters. In this case, the system achieves the steady state with the lowest possible dissipation rate compatible with the frustration pattern. The latter depends, however, on the initial state [21].

D. Discussion

We would like to underline and generalize two main results: First, due to particle rotations, dissipation rate decreases dynamically to reach its minimum in the steady state for a fixed driving *velocity*. We discussed the origin of dynamic minimization of dissipation to be a progressive increase of the number of NS contacts. In regular, but also in dense disordered granular systems, dissipation can arise only from the ''frustration'' of rotations. If the network of contacts and their states did not change, like in the case of regular systems studied here, then the evolution of the system would rapidly reduce the dissipation rate to its minimum possible value compatible with the geometry. In some circumstances, the dissipation rate can be virtually zero in the steady state when the driving velocity is constant, this essentially being due to friction with the walls. In other words, the point is not that ''particle rotations reduce dissipation rate in the system,'' as is generally argued about the role of rotations in granular systems. The problem has to somewhat be reversed. Particle rotations tend actually to reduce dissipation rate down to zero. The question then is to know why there *is* dissipation when a granular system is sheared. From

the foregoing discussion, we can state that ''frictional dissipation in granular systems is a consequence of disorder.'' In other words, due to disorder the network of contacts is reorganized during deformation. These rearrangements occur so frequently that the system does not have enough time to achieve its steady state, where the dissipation rate is weak.

Secondly, not only the global coefficient of friction, but also the inertia of the system can be renormalized to ''effective'' values which are independent of the applied force on the system for low and high values of the latter. The appearance of an effective inertia should not be specific to regular arrays. Variation of the friction force on the plane as a function of the linear acceleration of the system has its origin in NS contacts, where no dissipation takes place. At such contacts, the friction force is more and more mobilized as acceleration increases. Some of them reach the sliding limit and turn to sliding contacts. In this way, the number of NS contacts decreases with acceleration. We think that some particular features of granular media could be more conveniently explained in terms of an effective inertia. For instance, the nonharmonicity of sound propagation in granular media (those aspects not resulting from Hertzian contact law), could be an inertia effect [22]. Since the effective inertia seems to be higher in the quasistatic limit (low acceleration), physical consequences are expected to appear in slow deformations of granular systems as well. Large stress fluctuations observed in the flow of granular materials (near the orifice of a hopper, for example) could result from impulsions generated by the high effective inertia of the medium. These features are quite generic and are only quantitatively influenced by the parameters. For instance, the effective inertia increases with the particle-plane coefficient of friction, while the effective friction decreases at the same time. The interparticle coefficient of friction has an opposite effect. The coefficient of friction with each wall has only a limited effect on the rotation mode of the particle just in contact with it.

V. CONCLUSION

This work is an investigation of the influence of the nonsmoothness of contact laws on the global behavior of regular arrays of rigid particles. Its main objective is to make appear explicitly those features of granular systems which are difficult to observe or to identify in the context of geometrical disorder.

Our algorithm provides a vectorial representation of contact states in the system. Each contact is force-transmitting or nontransmitting, sliding or nonsliding. Contact states are determined in an iteration process simultaneously with contact forces and accelerations. The solution in dynamics is generally unique. However, in some circumstances, there may appear indeterminate states. We have identified the origins of such singularities and the degree of indeterminacy in each case. We have argued that in static equilibrium almost half of the contact forces inside the medium are undetermined.

During evolution, contact states change and achieve a steady state, where the accelerations of particles and contact forces stay constant in time. The steady state is independent of initial conditions. When the driving velocity is constant, the steady-state dissipation is the minimum possible value compatible with frustration of rotations. Since particle rotations lead to a very low dissipation in the steady state, we concluded that, in the general case of a dense disordered system, *disorder is the main reason why there is at all frictional dissipation in granular media*. In fact, due to geometrical disorder, contacts appear and disappear during time, so that the steady state is never reached by the system.

An interesting feature of the steady state is the appearance of collective rotation modes and contact states giving rise to length scales in between the system size and the size of the particles. These modes and the corresponding length scales are closely related to the progressive mobilization of friction forces inside the medium at nonsliding contacts.

In the steady state, the global friction force at the system-plane interface increases with the linear acceleration of the system. We have introduced a Legendre transformation on the friction force which allows for the definition of an effective inertia and an effective coefficient of friction. The effective inertia can be much higher than the total mass of the system in particular in the limit of weak acceleration. We argued that this property might be an important point to take into account for analyzing fluctuations observed in the granular flow.

ACKNOWLEDGMENTS

It is a pleasure to acknowledge many fruitful discussions with D. Wolf at HLRZ. This work has been supported by the European program of Human Capital and Mobility.

[1] E. Guyon, S. Roux, A. Hansen, D. Bideau, J. P. Troadec, and H. Crapo, Rep. Prog. Phys. **53**, 373 (1990).

[2] H. J. Herrmann, D. Stauffer, and S. Roux, Europhys. Lett. **3**, 265 (1987).

[3] T. Travers, D. Bideau, A. Gervois, and J. C. Messager, J. Phys. A **19**, L1033 (1986).

[4] L. Rothenburg and R. J. Bathurst, Géotechnique **39**(4), 601 (1989).

[5] F. Sidoroff, B. Cambou, and A. Mahboubi, Mech. Mater. **16**, 83 (1993).

[6] J. J. Moreau, Eur. J. Mech. A/Solids **13**, 4-suppl., 93 (1994).

[7] M. Jean, in *Mechanics of Geometrical Interfaces*, edited by A. P. S. Selvadurai, and M. J. Boulon (Elsevier, New York, 1995), pp. 463-486.

[8] M. Jean and J. J. Moreau, in *Proceedings of Contact Mechanics International Symposium*, edited by A. Curnier (Presses Univ. Romandes, Lausanne, 1992), pp. 31-48.

[9] P. D. Panagiotopoulos, *Inequality Problems in Mechanics and Applications* (Birkhäuser, Basel, 1985).

[10] *Disorder and Granular Media*, edited by D. Bideau and A. Hansen (Elsevier, New York, 1993).

[11] *Advances in the Mechanics and the Flow of Granular Materi-*

als, edited by M. Shahinpoor (Trans Tech, Clausthal, 1983).
[12] *Granular Matter*, edited by A. Mehta (Springer-Verlag, Berlin, 1993).
[13] H. M. Jaeger and S. R. Nagel, Science **255**, 1523 (1992).
[14] J. P. Bardet and Q. Huang, in *Powders and Grains 93*, edited by C. Thornton (A. A. Balkema, Rotterdam, 1993), pp. 39-43.
[15] G. M. Gere and S. P. Timoshenko, *Mechanics of Materials* (PWS-KENT, Boston, 1984).
[16] D. Bideau, A. Gervois, L. Oger, and J. P. Troadec, J. Phys. (Paris) **47**, 1697 (1986).
[17] W. H. Press, W. T. Vetterling, S. A. Teukolsky, and B. P. Flannery, *Numerical Recipes in Fortran* (Cambridge University Press, Cambridge, England, 1992).
[18] F. Radjai and S. Roux, Phys. Rev. E **51**, 6177 (1995).
[19] F. Radjai, P. Evesque, D. Bideau, and S. Roux, Phys. Rev. E **52**, 5555 (1995).
[20] C. S. Chang, in *Powders and Grains 93*, edited by C. Thornton (A. A. Balkema, Rotterdam, 1993), p. 105.
[21] L. Brendel and F. Radjai (unpublished).
[22] L. M. Schwartz, D. L. Johnson, and S. Feng, Phys. Rev. Lett. **52**, 831 (1984).